LAH 246

Cytometry 5:159–168 (1984)

Three-Color Immunofluorescence Analysis of Mouse B-Lymphocyte Subpopulations[1]

D. R. Parks, R. R. Hardy,[2] and L. A. Herzenberg

Department of Genetics, Stanford University School of Medicine, Stanford, California 94305

Received for publication October 17, 1983; accepted November 21, 1983

We have modified a fluorescence-activated cell sorter (FACS) to make three independent immunofluorescence measurements on each cell and used this system to study mouse B-lymphocyte subpopulations. An argon-ion laser (emitting at 488 nm) excites fluorescein- and phycoerythrin-labeled reagents, and a tunable dye laser charged with rhodamine 6G (emitting at 615 nm) excites an allophycocyanin-labeled reagent. We report simultaneous measurements of IgM, IgD, and the recently-defined mouse B lymphocyte antigens BLA-1 and BLA-2 on splenic lymphocytes of CBA/J mice and mice of the congenic strain CBA/N (which have an X-linked immunodeficiency [xid]). These data provide information on relationships among the B-cell populations in CBA/J "normal" mice and the defective CBA/N that could not be derived from one- or two-color immunofluorescent measurements. We believe this is the first use of allophycocyanin as an immunofluorescence label.

Key terms: Three-color FACS analysis, phycoerythrin, allophycocyanin, B lymphocytes, X-linked immunodeficiency

In our investigations of lymphoid cell subpopulations we have distinguished and sorted populations of cells that differ functionally even though there is no known cell surface marker that quantitatively defines the specific subpopulation. We distinguish these populations by the ratios of simultaneous quantitative measurements of two cell surface molecules on each cell.

Several systems employing one (18,22) or two lasers (23,27) have been used to make dual immunofluorescence measurements. Until recently, however, the possibilities for laser-based multiple immunofluorescence measurements have been limited by a shortage of suitable fluorochromes. The phycobiliproteins are a group of fluorescent compounds that are particularly promising as dyes to expand the array of fluorochromes available for immunofluorescence applications. Phycobiliproteins are auxiliary photosynthetic pigments of red algae and cyanobacteria (6). These proteins bear multiple chromophores which offer both novel spectral properties and the possibility of brighter fluorescent labeling than is possible with chromophores attached directly to an antibody or other ligand. One phycobiliprotein, phycoerythrin (PE), has been used previously as an immunofluorescent label (22), and we now report the use of a second, allophycocyanin (APC).

We have been using fluorescein (Fl) and Texas Red (TR) in our dual-laser system for some time (8,9,13). These, together with PE and APC, provide four immunofluorescent dyes that can be used in various combinations. Although it should be possible to use all four dyes in a two-laser excitation scheme, use of three at a time facilitates optimization of the individual measurements. We have excited fluorescein and PE with an argon-ion laser at 488 nm and excited APC with a tunable dye laser at 615 nm. In an accompanying article (19), Loken and Lanier report their findings using fluorescein, PE, and TR as dyes for three-color immunofluorescence. In addition, the combination of fluorescein, TR, and APC has advantages because there is a greatly reduced autofluorescence background in the TR and APC channels and because such a system permits live/dead discrimination using the fluorescent dead-cell label propidium iodide (PI).

Our previous two-color immunofluorescence analyses using a dual-laser fluorescence-activated cell sorter (FACS) have distinguished three populations of mouse B cells according to the amounts of surface IgM and IgD expressed per cell: population I, expressing high IgD and intermediate IgM levels, is predominant in most mice but is missing from a particular strain of immunodefective mice (CBA/N, X-linked immunodeficient mice); pop-

[1]This work supported in part by National Institutes of Health grants GM-17367 HD-01287 and CA-04681.

[2]R.R. Hardy is a junior fellow of the American Cancer Society, California Division (grant J-22-82).

ulation II, expressing high IgD and high IgM levels, is found at similar frequencies in all strains; and population III, expressing low IgD and high IgM levels, is found in spleen (but not in lymph nodes) and occurs at higher frequency in certain autoimmune strains (NZB) (8,9).

Further two-color analyses demonstrated that populations I, II, and III differentially express a series of lymphocyte cell surface proteins, including Ia, ThB, and, suprisingly, the pan T-cell antigen Ly-1 (13). Ly-1, formerly called Lyt-1, is present on a unique subpopulation of B cells (termed Ly-1 B) that comprises most of the cells in population III and is greatly expanded in NZB-related autoimmune mice (11,13). The distinctive surface characteristics, functional properties, organ location, and developmental pattern demonstrated for Ly-1 B cells suggest that this small subpopulation (and consequently most of population III) represents a separate lineage of B cells (12).

The lineage relationships of the remaining B cells (which constitute the vast majority of the Ig-bearing cells), however, are not well understood. There are two major theories concerning the lineage distinctions among these cells (28): (1) the single-lineage concept, in which a pre-B-cell population proceeds through several stages of increasing "maturity" and terminates in antibody-secreting cells (or memory cells); and (2) the branched-lineage concept, in which a precursor population divides into two (or more) branches that have functionally distinct response characteristics. We plan to approach this "lineage problem" by dividing B cells into subpopulations and then determining whether these subpopulations belong to a single lineage or instead constitute multiple lineages. Our two-color investigations with two recently-characterized monoclonal antibodies that mark subpopulations of B cells (53-10.1 and 30-E2) were sufficiently complex to necessitate quantitation of three cell surface markers simultaneously, so we have developed methods that enable us to make three simultaneous immunofluorescence measurements on a modified dual-laser FACS.

MATERIALS AND METHODS

Mice

CBA/J, CBA/N, and BALB/c mice were bred in our facility.

Monoclonal Antibodies

Rat anti-mouse IgM (clone 331-12) was produced by Dr. P. Kincade (15). Mouse monoclonal anti-IgD (specific for the "a" allotype, Igh-5^a) and rat monoclonal antibodies 53-10.1 (detecting the B-lymphocyte antigen BLA-1) and 30-E2 (detecting the B-lymphocyte antigen BLA-2) were all produced in this laboratory (16,21).

Immunoglobulin Labeling

Biotin (Bi)- and fluorescein (Fl)-labeling procedures have been described elsewhere (3,7). Reagents were conjugated at low label/protein ratios (F/P of 2–3) to minimize background staining. All reagents were stored at 4°C in 0.1% sodium azide, and deaggregated at 100,000g for 10 minutes in a Beckman Airfuge (Beckman Instrument, Palo Alto, CA) immediately before use.

Phycobiliprotein Conjugates

The PE-avidin conjugate was prepared by cross-linking the two proteins with N-succinimidyl 3-(2-pyridyldithio)propionate (4) and was generously provided by Dr. D. Rechtenwald (Becton Dickinson Monoclonal Center, Mountain View, CA). APC, extracted from the cyanobacterium *Anabaena variabilis*, was a gift of Dr. A.N. Glazer (University of California, Berkeley, CA). This protein was cross-linked to monoclonal antibody 53-10.1 by first labeling the dye protein with succinimidyl 4-(p-maleimidophenyl)butyrate (17) and then reacting it with 53-10.1 antibody that had been mildly reduced (using 20 mM dithioerythritol). Molecular weight analysis by high-performance liquid chromatography (TSK-250 column, Bio-Rad, Richmond, CA) showed that the conjugate consists primarily of one dye protein (110 kilodaltons [Kd]) coupled to a single IgG (150 Kd). The fluorescence excitation and emission spectra of the reagent were essentially identical to those of the APC alone.

Staining for FACS Analysis and Sorting

Single-cell suspensions (from which the erythrocytes had been lysed by 0.165 M ammonium chloride) were stained in microtiter wells as described previously (11). Green fluorescence was derived from directly conjugated Fl reagents, red fluorescence was obtained from APC-conjugated 53-10.1 antibody, and yellow fluorescence was obtained by using biotinated first step antibodies followed by PE-labeled avidin in a second incubation.

Laser Excitation

The 488-nm excitation is supplied by an argon-ion laser operating at 400 mW. The dye laser (Spectra Physics Model 375 Spectra Physics, Mountain View, CA) circulates rhodamine 6G, which is excited by a second argon-ion laser operating in all-lines mode (with most of the energy at 488 nm and 514.5 nm) and has useful output power from 575 nm to 630 nm. At 615 nm, as used here, it provides about 300 mW of output when excited with 2.5–3 W from the argon-ion laser. The dye laser output shows short-term fluctuation of about 1% RMS, which is comparable to that found with our argon-ion lasers. Once the system is warmed up (about 30 minutes), the output power of each laser remains essentially constant for over 4 hours.

Electronics

Signals from the "green" and "yellow" detectors were processed by dual compensator preamplifiers (18) to yield "true" Fl and PE signals. The "red" signal corresponds to APC without adjustment. All of the fluorescence signals were amplified with logarithmic amplifiers capable

of true logarithmic response over a range of 3.5 decades. Forward light scatter and the three fluorescence signals were peak-detected and digitized.

Computer Data Storage

Data from four measurement channels (forward light scatter and three immunofluorescences) were collected on a VAX11/780 computer (Digital Equipment, Maynard, MA) in list mode for sets of 10,000 or 30,000 cells (for controls or three-color stained samples, respectively). The programming for data acquisition, computation, and display was written in this laboratory by Mr. W. Moore.

Data Analysis

Two-color staining data are presented as "contour plots" that can be viewed as representations of three-dimensional surfaces in which the levels of green and red fluorescence per cell define the location of cells, and the frequency of cells at each location defines the "elevation" at that location. After interpolating and smoothing this surface, contour lines are drawn to represent different levels in the elevation (frequency). Various algorithms can be used to define the levels, resulting in different representations of a given data set. In the figures used here, the spacing between contours is chosen to give a selected fraction of the total number of cells in the region between adjacent contours ("probability" contours); the selected fraction is shown in the upper right corner of each figure panel. Three-color staining data has been analyzed by defining regions of interest on contour plots of forward light scatter versus one immunofluorescence (for example, BLA-1 staining). Contour plots of a second immunofluorescence (IgD staining) versus the third immunofluorescence (IgM staining) are then displayed for the cells in each region of interest (for example, BLA-1$^+$ cells) on the first plot. Histograms of each single parameter and counts of cells (integrations) in specific four-dimensional regions can also be produced.

RESULTS

Measurement System

System configuration. The measurements were carried out on a modified Becton-Dickinson cell sorter with a FACS-IV optical bench and FACS-II electronics. The optical configuration of the system is shown in Figure 1. Laser beams at 488 nm and 615 nm illuminate the liquid jet about 200 μm apart. The objective collects fluorescence from the laser intersection points and images it onto a mask with two apertures. Light from the 488-nm spot passes through one hole in the mask and is divided and filtered to yield green (515–560 nm) and yellow (560–600 nm) signals. Light from the 615-nm spot passes through the second hole in the mask and is reflected and filtered to give the red (635–680 nm) signal.

The lens behind the mask in the green/yellow channels (see Fig. 1) acts primarily as a field lens, imaging the principal plane of the objective onto the faces of the detectors. This assures that all light reaching the lens from the objective will fall within the sensitive area of the detectors and also distributes the signal over a region of optimum response near the center of each detector face.

Two more detectors (not shown in Fig. 1) are used to measure light scatter from the cells at 488 nm. Light scatter is detected in the forward direction by a standard diode detector, while large (obtuse) angle light scatter is collected by a fiber optic adjacent to the fluorescence objective and detected with a photomultiplier tube. We have found that large-angle light scatter is a very useful tool for distinguishing lymphocytes from macrophages and other granular cell types.

Signal-defining optics. The laser beams are focused by a single 50-mm-focal-length lens to spots with 40-μm diameter (at half maximum intensity) and with centers about 200 μm apart on the jet. The mask apertures are 3 mm square, corresponding to 130-μm wide regions on the jet.

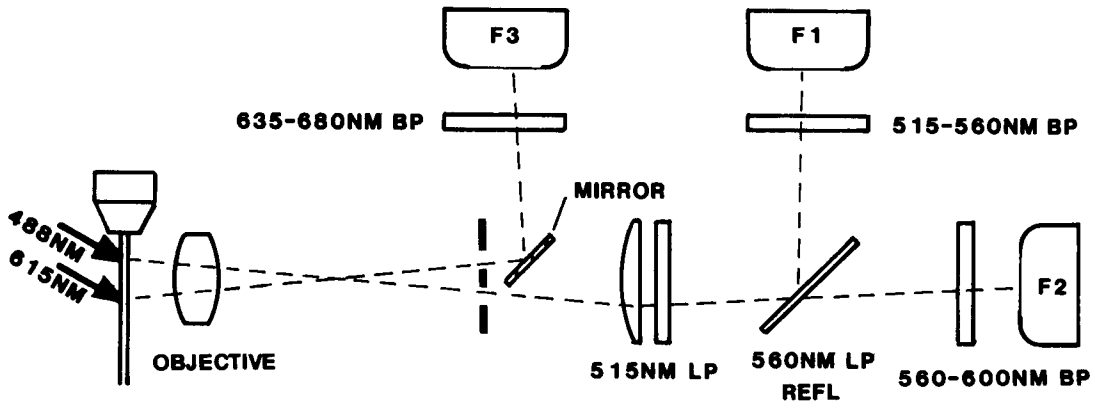

FIG. 1. Diagram of the optical configuration of the three-color immunofluorescence setup. The liquid jet, the laser beams, and the mask/mirror assembly have been rotated out of their actual orientation in order to allow the figure to be drawn in one plane.

System Test Results

Dyes and filters. The excitation and emission spectra of the dyes used in this study are shown in Figure 2. Fluorescein excites very well at 488 nm, while B-phycoerythrin (B-PE, from blue-green algae) excites there with about half of its peak efficiency (which is at 545 nm). Previous work with PE by Oi et al. (22) was done with R-phycoerythrin (R-PE, obtained from red algae), in which there is an additional excitation peak near 495 nm. R-PE is therefore much better for 488-nm excitation. Our use of B-PE was dictated by availability rather than choice of optimal spectral properties. We expect to use R-PE with the argon laser in the future. APC excites at nearly its maximum efficiency at 615 nm, while fluorescein and PE have essentially zero excitation efficiency at 615 nm. APC excites at only 3% of its peak efficiency at 488 nm.

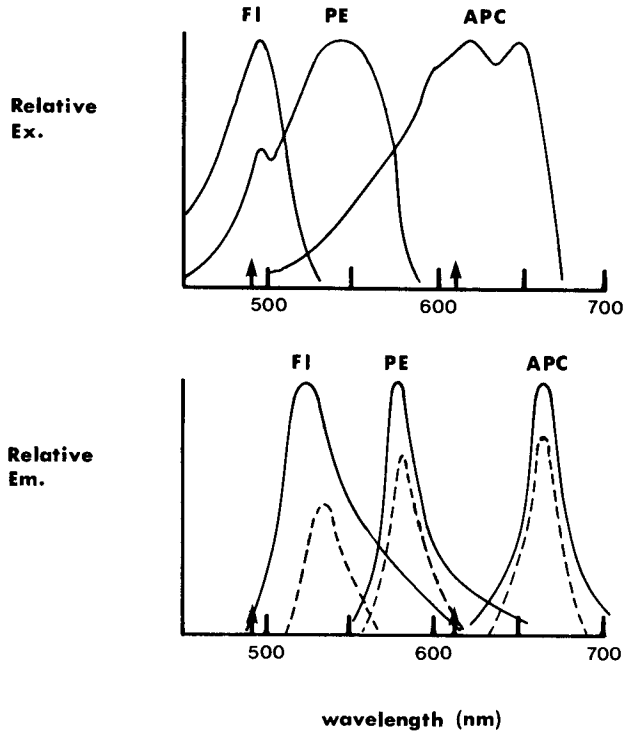

FIG. 2. Excitations (EX), emissions (EM), and filter acceptances (dashed curves under the corresponding emission spectra) of the fluorescent dyes used in this study. The argon-ion laser and dye laser wavelengths (488 nm and 615 nm, respectively) are marked with arrows.

The dashed lines under the emission spectra in Figure 2 show the part of the emitted light passed by the optical filters in each channel. In Table 1 the relative efficiencies of each filter set for the relevant dye emissions are presented. The only large correction required in the compensator-preamplifier is for the 560–600-nm ("yellow" channel) sensitivity to fluorescein emission. The green detector requires a small correction for its sensitivity to PE emission. Neither fluorescein nor PE is detectable on the APC detector.

Absolute fluorescence signal levels. To compare and evaluate the dyes and reagents we used in this study, we measured autofluorescence and cell staining with pairs of matched reagents in each measurement channel. The measurements were normalized for comparison to each other by calibrating the output signals in terms of a gain-independent standard: the number of "events" contributing to the measurement of each signal. This number corresponds roughly to the number of photoelectrons generated at the photomultiplier tube (PMT) cathode.

For a phenomenon based on summing independent events (such as counting a radiolabeled sample for a fixed time) the values obtained by repeated measurements on a single sample have a Poisson distribution. One characteristic of the Poisson distribution is that the square of the standard deviation (D^2) is equal to the mean number of events (N), i.e., $D^2 = N$. Thus, if we have one count on a radiolabeled sample, we can estimate the standard deviation of repeated counts or the confidence we have that the "real" count would be within a certain range of the single measurement. Conversely, in the present case we use the relation between the mean and standard deviation of a distribution produced by repeated measurements to estimate the mean in terms of Poisson events even though the measurement is taken in arbitrary units.

For uniform light pulses producing an average of N events contributing to the measurement, a mean output signal, $M = kN$, is produced, where k incorporates gains, etc., leading to the units used to quantitate M. In the measurement units the standard deviation, U, will be $U = kD$. The equations can be rearranged to give k and N in terms of the measured data: $k = U^2/M$ and $N = M^2/U^2$. We estimated the number of "events" required to

Table 1
Filter Transmission Efficiencies for Fluorescence Emissions From Several Dyes

Detection Channel[a]	Filter Bandpass	Fluorescein	Phycoerythrin	Allophycocyanin
Fl	515–560 nm	36%	3%	NA
PE	560–600 nm	13%	55%	NA
APC	635–680 nm	NA[b]	NA	58%

[a]Fl = fluorescein, PE = phycoerythrin, APC = allophycocyanin.
[b]Efficiencies labeled NA (not appropriate) are completely negligible in the FACS measurements because of the temporal and spatial separation of the two laser excitations.

produce a given signal in each measurement channel using a light-emitting diode (LED) source giving uniform light pulses of the same "shape" (time dependence) as the real cell-generated signals. Several data sets were recorded on each channel, using various neutral density filters to attenuate the LED signals. A linear fit to U^2 versus M of the data sets for each detector gives k for that measurement channel.

For fluorescences measured in our system, the standard deviation of small signal measurements is dominated by counting statistics of the photoelectrons produced at the PMT photocathode, and event estimates made as described above lead to numerical values (A − 1)/A times the photocathode electron count, where A is the electron amplification factor at each of the phototube dynodes (typically A is between 3 and 4). This event estimate is, however, exactly the value we want to use in comparing different signals and is the proper basis for estimating the precision of measurements on individual cells.

To make the reagent comparison, we labeled separate aliquots of a single original spleen cell sample with Bi-anti-Igh-5[a] followed by either Fl-avidin or PE-avidin; other aliquots were stained directly either with the Fl-53-10.1 or APC-53-10.1. The mean signal level of the logarithmic fluorescence data for positive staining populations was used in each case to represent the staining brightness. Cell autofluorescence estimates were made similarly using unstained hybridoma cells, which are larger and have more inherent autofluorescence compared with splenic lymphocytes.

The results are presented in Table 2. We detected larger signals from the fluorescein reagents than from the phycobiliprotein reagents in each case. Since experience in making phycobiliprotein reagents is still quite limited, we expect that the fluorescence yield of such reagents will be improved. Even with the current conjugates, APC shows a better real signal-to-autofluorescence ratio than fluorescein. This is due to the decrease in cell autofluorescence found with the longer wavelength excitation used to excite APC.

Test particles. We have found dye-labeled microspheres to be very useful for aligning and adjusting the three-color system. Fl and PE microspheres can be used to adjust the two-color compensator for these signals without the need for cells stained with each dye individually and without interference from cell autofluorescence in the adjustment. We have found TR-labeled microspheres to be adequate for aligning the APC channel.

The microspheres are carboxylated polystyrene about 1.3 μm in diameter (Polysciences, Inc., Warrington, PA, cat. #7760). These are quite nonfluorescent in their native state but can be labeled simply by incubation with fluorochrome-coupled proteins. We have found that such microspheres (noncovalently labeled with fluorochrome-conjugated avidin) are quite stable and can be stored frozen for later use. Immunoglobulins also stick to the microspheres, but not as well as avidin does. The phycobiliproteins themselves are acidic and do not stick to the carboxylated microspheres, but phycoerythrin-avidin is basic and adheres well.

Biological Results

The changes in expression of the BLA-1 and BLA-2 antigens during B-cell development suggest that the level of expression of both of these antigens is inversely related to the degree of B-cell maturity (see Table 3). Sites of less mature B cells (e.g., bone marrow) have more BLA-1- and BLA-2-positive B cells compared with

Table 2
Signal-Level Comparisons of Fluorescent Reagents and Cell Autofluorescences for the Three Fluorochrome/Detector Combinations Employed in This System[a]

	Reagents[b]					
	Number of Events			Relative Signal Level		
Dye	Avidin	Antibody 53-10.1	Autofl	Avidin	Antibody 53-10.1	Autofl
Fl	1,880	300	250	1.00	1.00	1.00
PE	208	ND	75	.11	ND	.30
APC	ND	50	28	ND	.17	.11

[a]Autofl = autofluorescence, Fl = fluorescein, PE = phycoerythrin, APC = allophycocyanin, ND = not done.
[b]Each "reagent" is the indicated binding specificity (avidin or antibody 53-10.1) labeled with the particular dye (Fl, PE, or APC) or autofluorescence measured under conditions appropriate for each dye; avidin is employed on cells stained with the same biotinated first step (anti-IgD). The "Number of Events," corresponding roughly to the number of photoelectrons producing the signal, was calibrated using a pulsed-light-emitting diode. For avidin and 53-10.1 the numerical value is for typical positive staining taken as the linear value corresponding to the mean of the log distribution of stained cells. Typical autofluorescence of a hybridoma line was derived similarly from the log fluorescence distribution of unstained live cells. The "Relative Signal Level" is the same data normalized to the signal for each reagent in the fluorescein channel. The measurements for each dye were made using excitation and detection conditions optimized for that dye in the three-color system.

Table 3
BLA-1 Marks Most B Cells in Bone Marrow But Few in Lymph Nodes[a]

Tissue	IgM^+ and—		IgM^- and—		Percent of IgM^+ Cells Bearing BLA-1
	$BLA\text{-}1^+$	$BLA\text{-}1^-$	$BLA\text{-}1^+$	$BLA\text{-}1^-$	
Bone marrow	5%	<1%	80%	14%	>90%
Spleen	15%	35%	1%	49%	30%
Lymph nodes	<1%	15%	<1%	>98%	<5%

[a]Cells were from adult (2–3-month-old) BALB/c mice.

Table 4
BLA-1 and BLA-2 Together Define Four Populations of B Cells in "Normal" Mice Such As CBA/J and BALB/c: One of These ($BLA\text{-}1^+2^-$) is Missing in CBA/N[a]

	Percentage of Splenic B Cells		
	CBA/N	CBA/J	BALB/c
$BLA\text{-}1^-,2^-$	30	45	64
$BLA\text{-}1^-,2^+$	51	25	9
$BLA\text{-}1^+,2^-$	1	14	17
$BLA\text{-}1^+,2^+$	17	16	9

[a]All cells were gated on IgM^+. All animals are between three and six months of age.

sites of more mature B cells (e.g., lymph nodes). In addition, studies of spleen cells from young mice support the idea that BLA-1 and BLA-2 are primarily expressed on immature or precursor B-cell populations, since most of the IgM^+ B cells in spleen express BLA-1 and BLA-2 at two weeks of age. As the mouse matures the frequency of BLA-1- and BLA-2-bearing cells among total splenic B cells decreases.

Simultaneous three-color immunofluorescence analysis provides considerable insight into the correlated expression of IgM, IgD, and BLA-1. Figure 3 presents BLA-1 versus forward light scatter contour plots, ungated except for large-angle scatter gating (to exclude macrophages), for CBA/J spleen cells from mice of two ages and for CBA/N adult spleen cells. The lower panels of the figure show IgM versus IgD staining of $BLA\text{-}1^-$ and $BLA\text{-}1^+$ cells defined by the rectangular gating regions shown in the BLA-1 versus scatter plots. The most striking feature that emerges in this comparison is the presence of an aberrant $BLA\text{-}1^-$ population in CBA/N mice that has a high level of surface IgM and a heterogenous level of surface IgD. On the other hand, the IgM-IgD pattern for the $BLA\text{-}1^+$ cells is similar in both types of mice. Thus the major difference in the IgM-IgD pattern noted previously by two-color analysis (8) occurs in the $BLA\text{-}1^-$ population. This suggests that the xid defect primarily affects the $BLA\text{-}1^-$ subpopulation of B cells. Further analyses of these data and their relation to the CBA/N defect have been published elsewhere (10).

Direct comparison of the correlated expression of BLA-1, BLA-2, and IgM on CBA/J and CBA/N B cells reveals further distinctions between normal and xid mice. As is shown in Figure 4, four populations of (IgM^+) B cells are found in CBA/J by such analysis: $BLA\text{-}1^+2^+$ cells, $BLA\text{-}1^-2^-$ cells, $BLA\text{-}1^+2^-$ cells, and $BLA\text{-}1^-2^+$ cells. A major difference between CBA/J and CBA/N is that the latter lack $BLA\text{-}1^+2^-$ cells. A second distinction is that these mice have fewer of the $BLA\text{-}1^-2^-$ B cells that constitute the predominant mature population in normal mice. The frequencies of these four populations of B cells found in normal (exemplified by CBA/J and BALB/c) and xid mice (CBA/N) are summarized in Table 4.

DISCUSSION

The three-color immunofluorescence detection system we have described can be used with several dye combinations, but with known dyes at least one must be a phycobiliprotein in order to obtain two immunofluorescence signals from single wavelength excitation by one of the lasers. We have employed fluorescein/phycoerythrin/allophycocyanin because the long wavelength excitation of APC gives good separation from PE detection, although with bright-staining reagents (and different filters) Texas Red can replace APC (19). We have also obtained measurements similar to those discussed above (data not shown) using a Fl/TR/APC triple-immunofluorescence system in which TR and APC are both excited by the dye laser at 590 nm. One advantage of this system is that propidium iodide live/dead discrimination (5) can be added as a second fluorescence excited by the 488-nm argon laser. The use of 590-nm excitation for two of the immunofluorescences may help to reduce the problem of cell autofluorescence and thereby increase the separation between stained and unstained cells. Otherwise, the choice between this and the Fl/PE/APC system would depend on the availability and quality of TR and PE reagents.

Relative signal levels of the phycobiliprotein dyes are currently not as high as predicted from theoretical considerations of the number of bilin groups per staining reagent (6). This may be due to the coupling method or to an as yet unrecognized problem and is currently under intensive study. A generalized coupling method that yields stable one-to-one complexes of dye protein and immunoglobulin is an important goal in making this technology widely available. Clearly it is important to avoid making protein complexes with nonspecific binding properties.

Another important complication that may occur when working with two immunofluorescences derived from a single-wavelength excitation is the possibility of energy

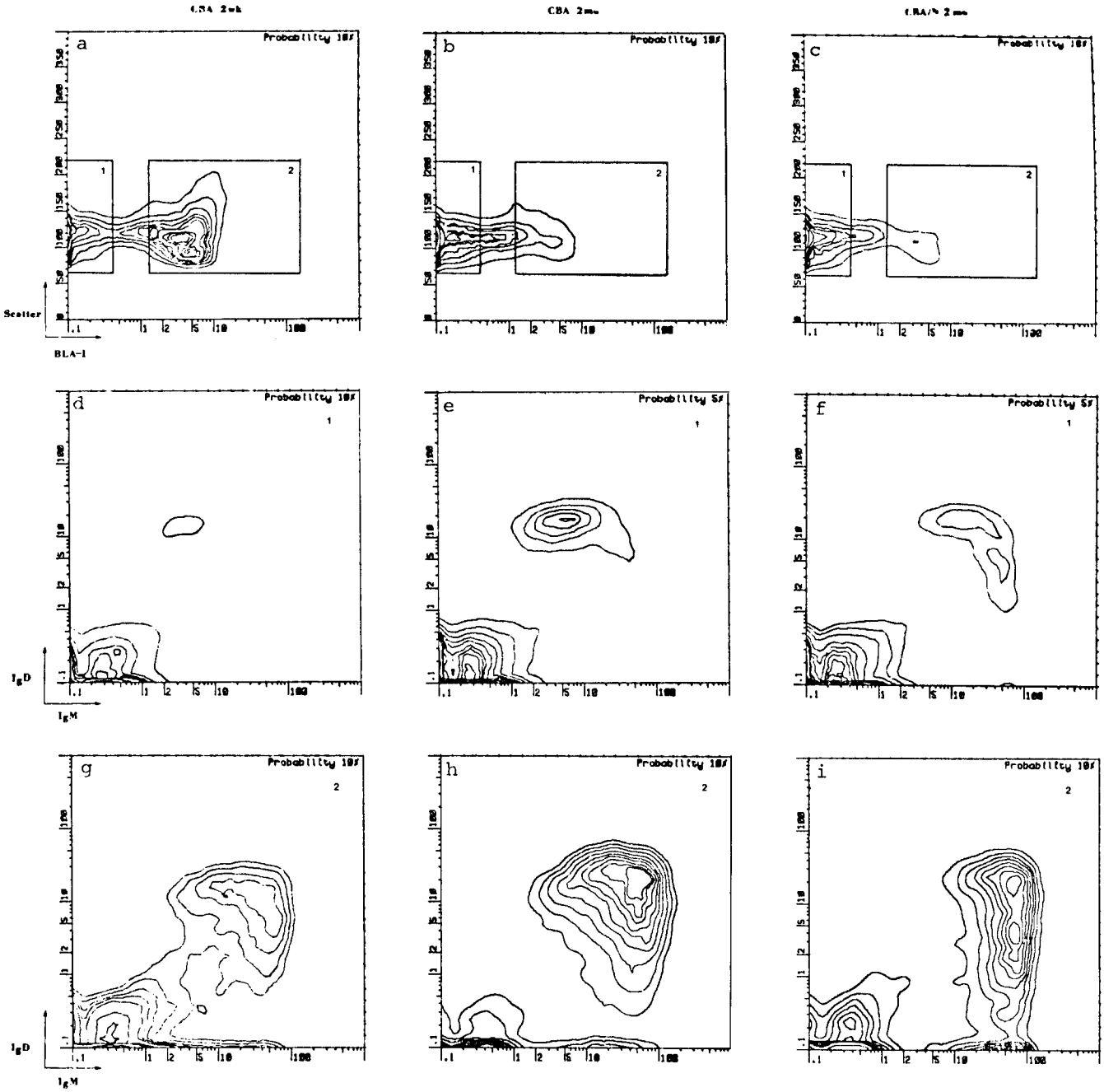

FIG. 3. Three-color simultaneous flow cytofluorometric analysis of IgM, IgD, and BLA-1 shows that the major difference in the IgM-IgD patterns of the splenic lymphocytes from normal and X-linked immunodeficient (xid) mice resides in a subpopulation (BLA-1$^-$) of B cells. In contrast, the BLA-1$^+$ B cells have a similar IgM-IgD pattern in young, adult, and immunodefective mice. The top panels are contour plots of BLA-1 staining versus forward scatter for spleen cells from (a) two-week-old CBA/J (young normal) (b) two-month-old CBA/J (adult normal) and (c) two-month-old CBA/N (adult xid) mice. The two rectangular regions marked on each of these plots are used to produce the IgM versus IgD contour plots for BLA-1-negative (panels d–f) and BLA-1-positive cells (panels g–i). The probability level used in contour definition was adjusted in some cases to compensate for the large number of non-B cells in the BLA-1$^-$ gating region.

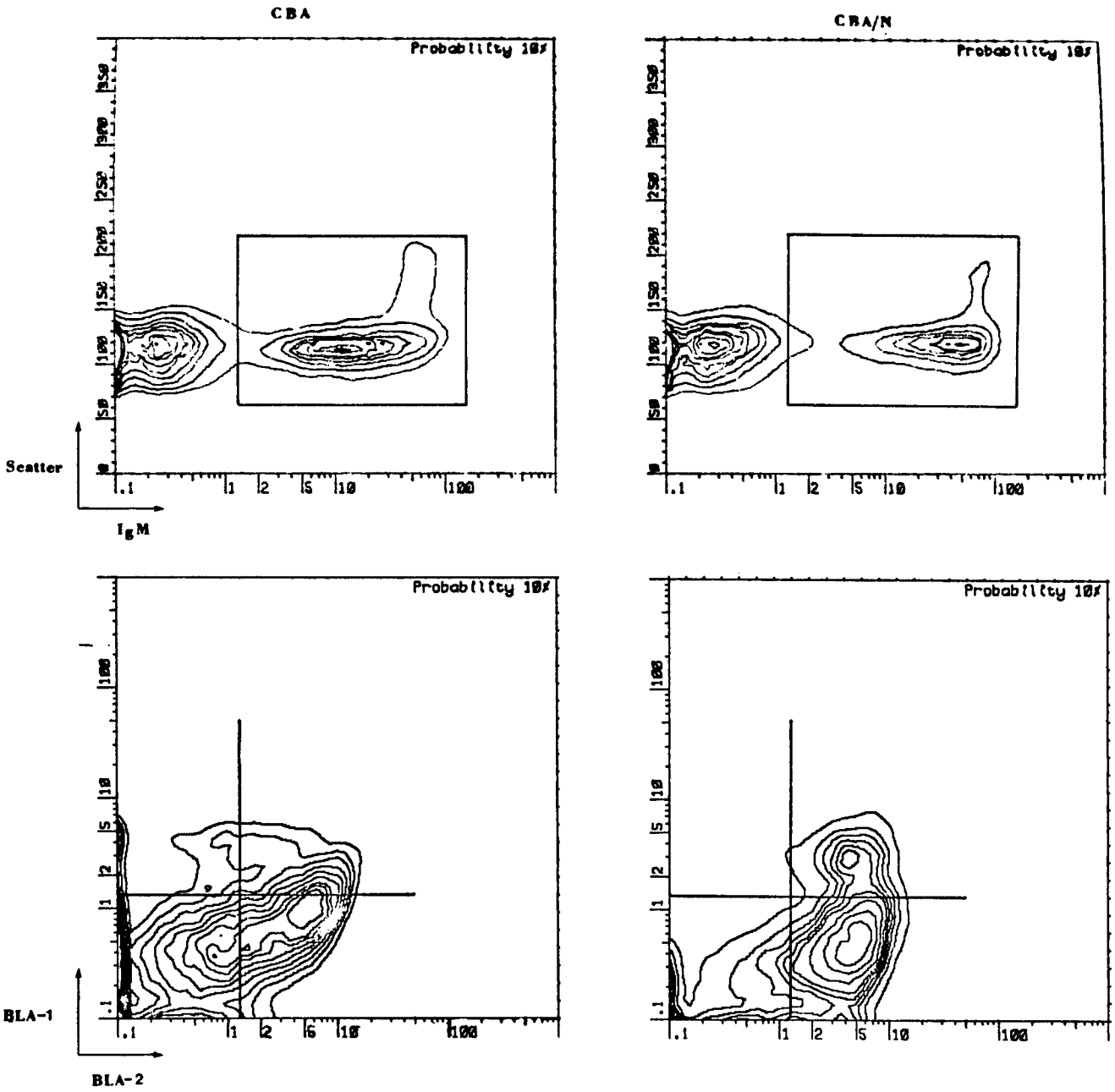

FIG. 4. Three-color simultaneous immunofluorescence analysis for IgM, BLA-1, and BLA-2 shows that the correlated measurements of BLA-1 and BLA-2 define four populations of IgM^+ spleen cells, one of which is missing from mice that carry the X-linked immune deficiency. The top panels are contour plots of IgM staining versus forward light scatter for spleen cells from two-month-old CBA/J (normal) and two-month-old CBA/N (xid) mice. The regions boxed in the top panels (IgM^+ cells) are then used to produce the BLA-1 versus BLA-2 contour plots (shown in the lower panels).

transfer from the shorter-wavelength reagent to the longer-wavelength reagent due to overlaps in their emission and excitation spectra (2). This would be noted primarily as a reduction in fluorescence intensity of the shorter-wavelength stain. To date, we have searched for but not observed such transfer between Fl and PE on separate staining reagents bound to cellular determinants. However, it is clear that if the dye molecules approach each other to within a certain distance, such transfer will occur. Careful controls showing that each stain in a mixture of reagents gives the same fluorescence profile as when the reagent is employed individually are needed to ensure that energy transfer is not taking place. Alternatively, if energy transfer does take place, it can be used to give some indication of distances between two cell surface determinants.

The biological data presented here comparing the correlated expression of BLA-1, BLA-2, and IgM on CBA/J and CBA/N (xid) spleen cells demonstrate the existence of four (IgM-bearing) B-cell populations: one of these lacks both BLA-1 and BLA-2 and includes the predominant, mature, resting B-cell population in normal mice; the second expresses both antigens and appears to include B cells that migrated most recently from bone marrow to spleen (and have not as yet lost BLA-1 or BLA-2). Although both of these populations are present in all mice to some extent, xid animals have fewer of the double-negative population.

Two other B-cell populations are present in normal mouse spleen: one expresses BLA-1 but lacks BLA-2, and the other expresses BLA-2 but lacks BLA-1. The former population ($BLA\text{-}1^{+}2^{-}$) is missing in xid mice. If, as we suspect, these populations represent cells in transition from the immature ("precursor") stage to the mature ("terminal") resting B-cell stage, then the absence of one of these from xid mice suggests the existence of two distinct B-cell lineages and that xid mice lack the lineage that loses BLA-2 before it loses BLA-1. The lack of this lineage would also account for the observation of fewer mature ($BLA\text{-}1^{-}2^{-}$) cells in CBA/N.

Previous studies have suggested that xid animals lack a distinct lineage of B cells (1,14). CBA/N mice clearly have a deficit of the mature B cells found in normal animals and have a constellation of functional immune impairments associated with this defect including a failure to make antibody to certain T-independent (TI-2) antigens (20,24–26). A two-lineage model of B-cell development has interesting implications, considering the functional defects found in xid animals. For example, since xid mice do not respond to TI-2 antigens, the missing lineage in these mice could be required for response to such antigens.

In summary, three-color immunofluorescence with phycobiliprotein-conjugated reagents opens up a new era in flow cytometry. The ease with which we can now simultaneously quantitate the amounts of two, three, and even four cell surface molecules will provide important means for studying complex cell populations. One obvious application is to the study of the complex mixture of cells which constitute the immune system [demonstrated here and in the accompanying paper by Loken and Lanier (19)]. We can expect to find currently unrecognized subpopulations of cells as we carry out further three- and four-color immunocytofluorometric analyses.

ACKNOWLEDGMENTS

We thank Dr. A. Glazer of the University of California, Berkeley, for purified allophycocyanin and Dr. D. Rechtenwald of the Becton Dickinson Monoclonal Antibody Center for PE-labeled avidin. Mr. H. Takahashi and Ms. L. Peterson provided expert technical assistance with cell isolation and staining. Mr. R. Stovel and Mr. T. Nozaki carried out much of the engineering and electronic design on the FACS system. Mr. W. Moore wrote the VAX computer data-handling programs and worked out the statistical basis for the absolute fluorescence signal estimates. Dr. K. Hayakawa and Dr. L.A. (Lee) Herzenberg provided important help and discussion.

LITERATURE CITED

1. Ahmed A, Scher I, Sharrow SO, Smith AH, Paul WE, Sachs DH, Sell KW: B lymphocyte heterogeneity: Development of an alloantiserum which distinguishes B lymphocyte differentiation antigens. J Exp Med 145:101, 1977.
2. Barber DJW, Richards JT: Energy transfer in the accessory pigments R-phycoerythrin and C-phycocyanin. Photochem Photobiol 25:565, 1977.
3. Bayer EA, Wilcheck M: The avidin-biotin complex as a tool in molecular biology. Trends Biochem Sci 3 (Nov):N257, 1978.
4. Carlsson J, Drevin H, Axen R: Protein thiolation and reversible protein-protein conjugation. N-Succinimidyl 3-(2-pyridyldithio) propionate, a new heterobifunctional reagent. Biochem J (Tokyo) 173:723, 1978.
5. Dangl JL, Herzenberg LA: Selection of hybridomas and hybridoma variants by the fluorescence activated cell sorter. J Immunol Methods 52:1, 1982.
6. Glazer AN: Phycobilisomes: Structure and dynamics. Annu Rev Microbiol 36:173, 1982.
7. Goding J: Conjugation of antibodies with fluorochromes. Modification to standard methods. J Immunol Methods 13:215, 1976.
8. Hardy RR, Hayakawa K, Haaijman J, Herzenberg LA: B cell subpopulations identified by two-color fluorescence analysis. Nature 297:589, 1982.
9. Hardy RR, Hayakawa K, Haaijman J, Herzenberg LA: 1982. B cell subpopulations identifiable by two-color fluorescence analysis using a Dual-Laser FACS. In: Immunoglobulin D: Structure and Function, Vol 399, Thorbecke GJ, Leslie GA (eds). Annals of the New York Academy of Science, New York, pp 112–121.
10. Hardy RR, Hayakawa K, Parks DR, Herzenberg LA: Demonstration of B-cell maturation in X-linked immunodeficient mice by simultaneous three-colour immunofluorescence. Nature 306:270, 1983.
11. Hayakawa K, Hardy RR, Parks DR, Herzenberg LA: The "Lyl B" cell subpopulation in normal, immunodefective and autoimmune mice. J Exp Med 157:202, 1983.
12. Hayakawa K, Hardy RR, Herzenberg LA, Steinberg AD, Herzenberg LA: Ly-1 B: A functionally distinct B cell subpopulation. In: Progress in Immunology, Proceedings of the 5thInternational Congress of Immunology, Kyoto, Japan, August, 1983, Tada T, Yamamura, Y. (eds.) Academic Press, New York, 1983 (in press).
13. Herzenberg LA, Hayakawa K, Hardy RR, Tokuhisa T, Oi VT, Herzenberg LA: Molecular, cellular and systemic mechanisms for regulating IgCH expression. Immunol Rev 67:5, 1982.
14. Huber B, Gershon RK, Cantor H: Identification of a B cell surface structure involved in antigen-dependent triggering: Absence of this structure of B cells from CBA/N mutant mice. J Exp Med 145:10, 1977.
15. Kincade PW, Lee GW, Sun L, Watanabe T: Monoclonal rat antibodies to murine IgM determinants. J Immunol Methods 42:17, 1981.
16. Ledbetter JA, Herzenberg LA: Xenogeneic monoclonal antibodies to mouse lymphoid differentiation antigens. Immunol Rev 47:63, 1979.
17. Lee ACJ, Powell JE, Tregear GW, Niall HD, Stevens VC: A method for preparing β-hCG COOH peptide-carrier conjugates of predictable composition. Mol Immunol 17:749, 1980.
18. Loken MR, Parks DR, Herzenberg LA: Two-color immunofluorescence using a fluorescence-activated cell sorter. J Histochem Cytochem 25:899, 1977.
19. Loken MR, Lanier LL: Three color immunofluorescence analysis of Leu antigens on human peripheral blood using two lasers on a fluorescence activated cell sorter. Cytometry 5:152–159, 1984.
20. Mosier DE, Zitron IM, Mond JJ, Ahmed A, Scher I, Paul WE: Surface immunoglobulin D as a functional receptor for a subclass of B lymphocytes. Immunol Rev 37:89, 1977.
21. Oi VT, Jones P, Goding JW, Herzenberg LA, Herzenberg LA: Properties of monoclonal antibodies to mouse Ig allotypes, H-2 and

Ia antigens. Curr Topics Microbiol Immunol 81:115, 1978.
22. Oi VT, Glazer AN, Stryer L: Fluorescent phycobiliprotein conjugates for the analysis of cells and molecules. J Cell Biol 93:981, 1982.
23. Parks DR, Hardy RR, Herzenberg LA: Dual immunofluorescence—New frontiers in cell analysis and sorting. Immunol Today 4:145, 1983.
24. Scher I, Steinberg AD, Berning AK, Paul WE: X-linked B-lymphocyte immune defect in CBA/N mice. II. Studies of the mechanisms underlying the immune defect. J Exp Med 142:637, 1975.
25. Scher I, Sharrow SO, Paul WE: X-linked B-lymphocyte defect in CBA/N mice. III. Abnormal development of B-lymphocyte populations defined by their density of surface immunoglobulin. J Exp Med 144:507, 1976.
26. Subbarao B, Ahmed A, Paul WE, Scher I, Lieberman R, Mosier DE: Lyb7, a B cell alloantigen controlled by genes linked to the IgCh locus. J Immunol 122:2279, 1979.
27. Titus JA, Haugland R, Sharrow SO, Segal DM: Texas Red, a hydrophilic, red-emitting fluorophore for use with fluorescein in dual-parameter flow microfluorometric and fluorescence microscopic studies. J Immunol Methods 50:193, 1982.
28. Wortis HH, Burkly L, Hughes D, Roschelle S, Waneck G: Lack of mature B cells in nude mice with X-linked immune deficiency. J Exp Med 155:903, 1982.